Van Paepegem, W. and Degrieck, J. (2001). Fatigue Degradation Modelling of Plain Woven Glass/epoxy Composites. *Composites Part A*, 32(10), 1433-1441.

Fatigue Degradation Modelling of Plain Woven Glass/epoxy Composites

W. Van Paepegem* and J. Degrieck

Ghent University, Dept. of Mechanical Construction and Production,
Sint-Pietersnieuwstraat 41, 9000 Gent, Belgium

Abstract

Due to their anisotropic and inhomogeneous nature, the fatigue behaviour of fibre-reinforced composite materials is complicated and since many years a large research effort is being spent on this problem. Despite of these efforts, fatigue design of fibre-reinforced composites still has to rely mostly on expensive time-consuming fatigue experiments and large safety factors have to be adopted. In this paper a combined experimental/numerical investigation of the fatigue behaviour of plain woven glass/epoxy composites is presented. Bending fatigue tests were used to yield the experimental data. With the aid of an advanced phase-shift shadow Moiré technique, an out-of-plane displacement profile during fatigue life of the composite specimens was recorded at a number of intervals, as well as the bending force history. A residual stiffness model which describes the fatigue damage behaviour of the composite material, was adopted. Next a new finite element approach was developed to implement the fatigue damage model in a commercial finite element code that proves to be capable of simulating the observed experimental results.

Keywords: A. Polymer-matrix composites (PMCs), B. Fatigue, C. Finite element analysis, C. Damage mechanics.

1. Introduction

Fibre-reinforced composite materials are extensively used in aerospace structures, naval industry and other high-tech designs, because of their high specific stiffness and strength. Although the fatigue behaviour of fibre-reinforced composites has been studied since many years, it is still not possible to make adequate predictions about the fatigue life and the degradation of stiffness and strength without extensive 'ad hoc' investigation.
Reliable numerical simulations would result in large savings in budget and time. Moreover the implementation of the fatigue models in a finite element code is indispensable in order to apply them to the simulation of full-scale structural composite components. With composites the variety of fibre reinforcements used (glass, carbon, aramid, ...) and the influence of the stacking sequence require that the damage model should be intrinsic to the material considered and should not depend on boundary conditions, material lay-up, ...
The presented results concern the fatigue behaviour of plain woven glass/epoxy composites. Bending fatigue experiments are used to provide the necessary experimental input. Since strain gauges and a digital phase-shift shadow Moiré technique are applied, the experimental results yield very valuable information for the development of the fatigue damage model. Next a new finite element approach is dedicated to validating the proposed fatigue damage model against the data measurements.

* Corresponding author (Fax: +32-(0)9-264.35.87, E-mail: Wim.VanPaepegem@rug.ac.be).

2. Experimental procedures

2.1. Materials

As mentioned, the material used in this study was a glass fabric/epoxy composite. The fabric was a Roviglass R420 plain-woven glass fabric (Syncoglas) and the epoxy was Araldite LY 556 (Ciba-Geigy). The plain woven glass fabric was stacked in eight layers and two different stacking sequences were used: the first type is denoted as $[\#0^o]_8$, where '0°' means that the warp direction of each of the eight layers has been aligned with the loading direction and where the symbol '#' refers to the fabric reinforcement type, while the angle between the warp direction of all layers of the second type and the loading direction is 45º (denoted as $[\#45^o]_8$). All composite specimens were manufactured using the resin-transfer-moulding technique. After curing they had a thickness of 2.72 mm. The samples were cut to dimensions of 145 mm long by 30 mm wide on a water-cooled diamond saw. The fibre volume fraction V_f was 0.48.
The in-plane elastic properties of the $[\#0°]_8$ composite laminates were determined using the dynamic modal analyis method described by Sol et al. [1,2]. They are listed in Table 1.

Table 1 Measured in-plane elastic properties of the $[\#0°]_8$ composite laminates

E_{11} (GPa)	24.57
E_{22} (GPa)	23.94
ν_{12} (-)	0.153
G_{12} (GPa)	4.83

2.2. Testing procedure

Although fatigue experiments in pure tension and compression are most often used in fatigue research [3-5], bending fatigue experiments were preferred because they allow to test the finite element implementation in more complicated and hence more realistic conditions [6-8]. Figure 1 shows the experimental setup for displacement-controlled bending fatigue tests.

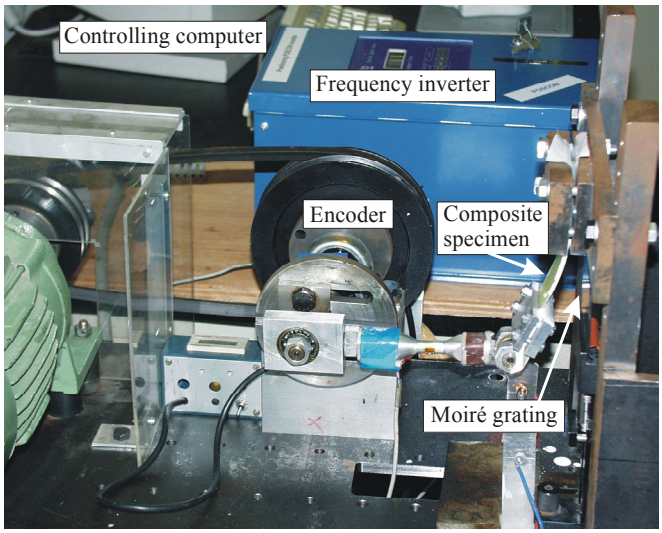

Figure 1 Experimental bending fatigue setup.

A schematic drawing of the setup is shown in Figure 2.

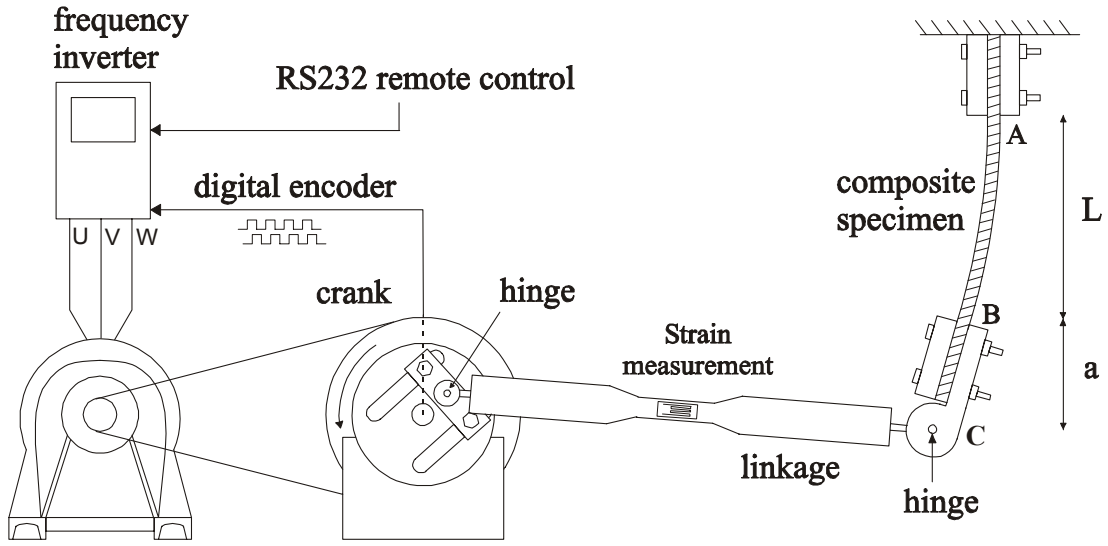

Figure 2 Schematic drawing of the experimental setup for bending fatigue.

The outcoming shaft of the motor has a rotational speed of 185 rpm. The power is transmitted by a V-belt to a second shaft, which provides a fatigue testing frequency of 2.2 Hz. The influence of frequency can be assumed small in this range of values (Manger et al. [9]). The power transmission through the V-belt ensures that the earthing of the motor and the earthing of the measurement system are electrically isolated, which is an advantage mainly with metallic or carbon fibre-reinforced specimens.

The second shaft bears a crank-linkage mechanism, which imposes an alternating displacement on the hinge (point C) that connects the linkage with the lower clamp of the composite specimen. At the upper end the specimen is clamped. Hence the sample is loaded as a composite cantilever beam. The amplitude of the imposed displacement is a controllable parameter and the adjustable crank allows to choose between single-sided and fully-reversed bending, i.e. the deflection can vary from zero to the maximum deflection in one direction, or in two opposite directions, respectively.

To record the out-of-plane displacement profile in the maximum deformed state, it was necessary to develop a mechanism to hold the specimen fixed in this state, because recording the profile while the test keeps running at a frequency of 2.2 Hz, gives rise to some practical problems. A rotary digital encoder was attached to the second shaft. Its angular position (relative to a certain reference angle) is directly related with the loading path of the composite specimen. The frequency inverter reads the signal from the rotary encoder and can stop and hold the motor at a predetermined angular position of the encoder. The commands for the inverter are controlled by a computer and sent through a RS232 communication line. This mechanism allows the phase-shift shadow Moiré method, which will be outlined below, to be used with this bending fatigue setup.

3. Digital phase-shift shadow Moiré method

Moiré techniques are straightforward methods for contactless non-destructive metrological measurements. Moiré topography in particular is a widely used means for shape contouring of three-dimensional objects. In general Moiré topography can be classified into two main categories: projection Moiré and shadow Moiré, according to the optical arrangement used.
In the case of a standard shadow Moiré system, a grating is positioned close to the object and its shadow is observed through the grating. A great deal of supplementary information in the gray level variation can be revealed by using the phase-shift method. The phase-shift is obtained by changing the object-to-grating distance [10,11]. In Figure 3, the standard shadow Moiré setup is shown. The light source and the observer are assumed to be pointlike and are placed at a finite distance from the grid.

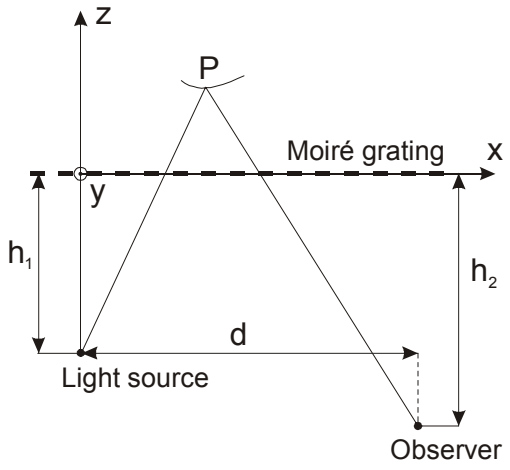

Figure 3 Moiré contouring system with light source and observer at finite distance from the grating.

If and only if the light source and the observer are placed at the same distance from the grating (i.e. $h_1 = h_2$), a term is produced in the fringe pattern which is solely dependent on z [12]. However the z-displacements can be obtained far more accurately when introducing phase-shifts. With each phase-shift the object-to-grating distance is changed with a shift δ_k (k = 1,...,m) in the z-direction. The standard procedure for the phase-shift shadow Moiré method is based on the following equations [13]:

$$I_k(x,y) = A(x,y) + B(x,y)\cdot\cos\left(\frac{2\pi d(z+\delta_k)}{ph}\right) \qquad \delta_k = \frac{k-1}{m}\cdot\frac{ph}{d} \tag{1}$$

where $I_k(x,y)$ is the fringe pattern for the k-th shift, d is the distance between the light source and the observer, h ($h = h_1 = h_2$) is the distance between the grating and the light source and observer, p is the pitch of the Moiré grating and A(x,y) and B(x,y) are the background and local contrast respectively. When solving the system in Equation (1) with the Gaussian least squares approach, the general solution for the interference phase distribution $\Delta\phi(x,y)$ with m phase-shifts ($m \geq 3$) is [14]:

$$\Delta\phi(x,y) = \arctan\frac{-\sum_{k=1}^{m} I_k(x,y)\sin\left(\frac{2\pi}{m}(k-1)\right)}{\sum_{k=1}^{m} I_k(x,y)\cos\left(\frac{2\pi}{m}(k-1)\right)} \tag{2}$$

The out-of-plane displacement is then given by:

$$z(x,y) = \frac{ph}{d} \cdot \frac{\Delta\phi(x,y)}{2\pi} \tag{3}$$

This common procedure has serious disadvantages in this case. At least three and better five phase-shifts are required to solve for the unknown background contrast A(x,y), local contrast B(x,y) and interference phase distribution $\Delta\phi(x,y)$. Hence, every time that the fatigue test is stopped to record the out-of-plane displacement profile, five phase-shifts should be performed. Since the measurement procedure should be automated (to keep the fatigue tests running day and night), an accurate set of computer-controlled phase-stepping devices would be required. Therefore a digital phase-stepping technique has been developed by the authors to reconstruct the out-of-plane displacement profile from only one image.
The purpose of the digital phase-shift shadow Moiré method is to capture only one image and to perform the phase-shifts numerically. The reference grating is placed in the illumination path only, and the digital camera captures the image of the projection onto the deformed object surface of the reference grating lines. Due to the simple optical arrangement, the errors caused by optical settings are eliminated. A typical image is shown in Figure 4.

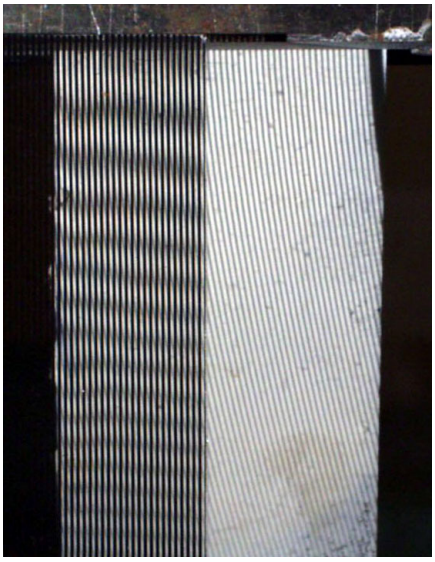

Figure 4 Moiré fringes (left) and projection onto the specimen of the reference grating lines (right).

After the image is captured, a virtual reference grating is created with the same pitch as the reference grating used in the experimental setup. Because the digital images are grabbed with a CCD-camera, which is in fact an observer at a finite distance from the grid, the virtual transmission function of the grid has to be corrected for the fact that both the observer and the light source are not at infinity [12].

4. Experimental results

Fatigue experiments were performed with different values of the imposed displacement, as well as with single-sided and fully-reversed bending. To characterize each experiment, the

'displacement ratio' $R_d = \frac{u_{min}}{u_{max}}$ (analogous to the stress ratio R) is defined, whereby the minimum deflection is not necessarily zero. When the displacement u_{max} and the length L between the both clamps (Figure 2) are further given too, all parameters of the fatigue experiment are known.

Figure 5 shows the force-cycle history for a $[\#0°]_8$ and $[\#45º]_8$ specimen, subjected to single-sided bending with u_{max} = 34.4 mm. The abscissa contains the number of cycles; the ordinate axis shows the force (Newton), which is measured by a strain gauge bridge (Figure 2) during the fatigue tests.

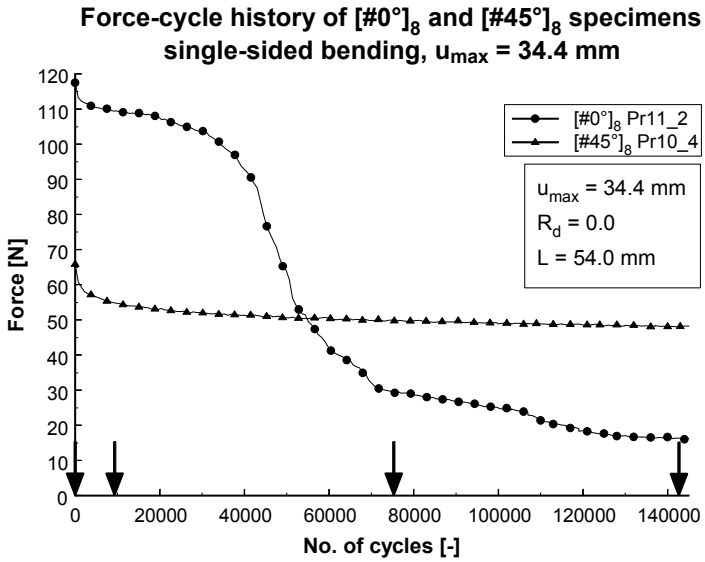

Figure 5 Force-cycle histories for $[\#0°]_8$ and $[\#45°]_8$ specimens (single-sided bending, u_{max} = 34.4 mm).

The arrows in Figure 5 indicate the cycle numbers (N = 1; 9,000; 67,682; 142,540), where an out-of-plane displacement profile of the specimens has been recorded by means of the digital phase-shift shadow Moiré method. These shapes are shown in Figure 6 for the $[\#0°]_8$ specimen and in Figure 7 for the $[\#45°]_8$ specimen respectively. It is clearly demonstrated that the fatigue behaviour of both specimen types is very different. With regard to the $[\#0°]_8$ specimen, a hinge is formed at the clamped cross-section (which corresponds with the sharp decline in the force-cycle history in Figure 5) and the strains in the parts remote from the fixation are nearly reduced to zero. On the other hand the out-of-plane displacement profile of the $[\#45°]_8$ specimen remains nearly the same, as well as the force necessary to impose the bending displacement (Figure 5).

The small ripples in the curves correspond to very small inegalities of the specimen surface, which are due to the coat of paint on the surface.

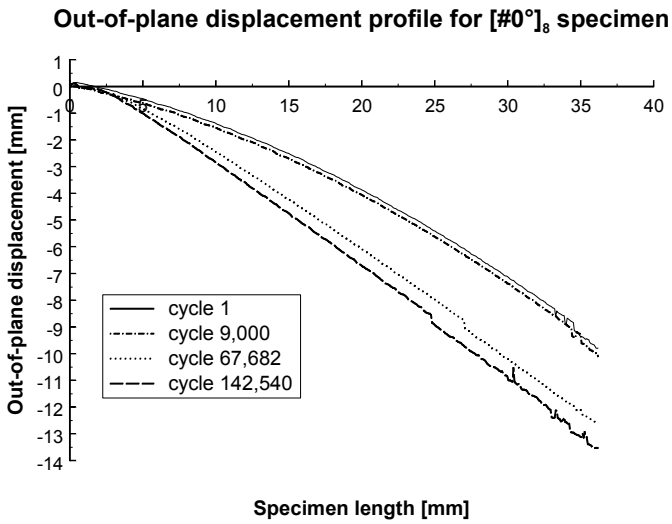

Figure 6 Out-of-plane displacement profile for $[\#0°]_8$ specimen.

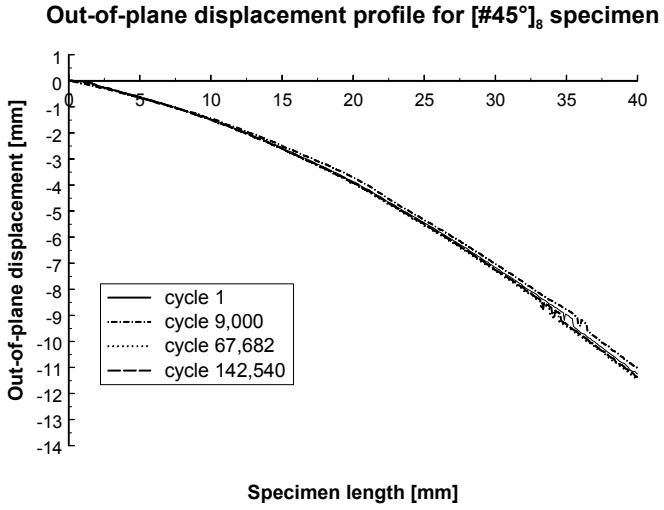

Figure 7 Out-of-plane displacement profile for $[\#45°]_8$ specimen.

When the imposed displacement u_{max} increases to 39.0 mm, the decline for the $[\#0°]_8$ specimens is even more pronounced, as can be seen in Figure 8. Figure 9 shows that the deterioration for $[\#45°]_8$ specimens is now also severe, but remains far more gradual.

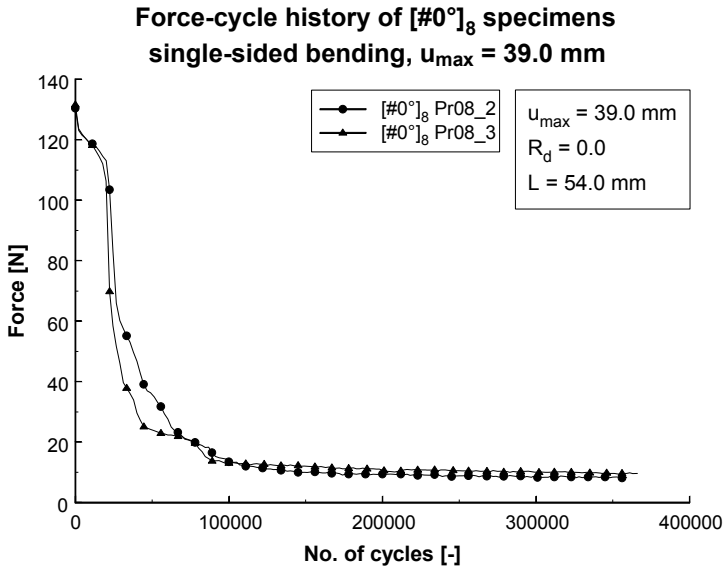

Figure 8 Force-cycle histories for $[\#0°]_8$ specimens (single-sided bending, u_{max} = 39.0 mm).

Although the scatter in the fatigue experiments is limited, small deficiencies in the mechanical properties can make the difference between complete failure and a steady-state condition. Indeed, the force-cycle paths of the three $[\#45°]_8$ specimens in Figure 9 start to diverge after a few thousands of cycles and the fatigue performance of the 'Pr06_4' specimen is in the end a lot better than that of the 'Pr06_5' specimen.

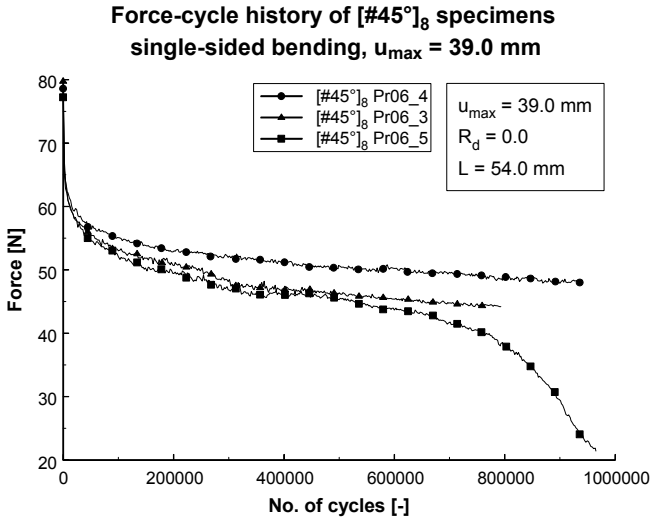

Figure 9 Force-cycle histories for $[\#45°]_8$ specimens (single-sided bending, u_{max} = 39.0 mm).

Finally, Figure 10 shows an experiment with fully-reversed bending (R_d = -1.0). Although the imposed displacement u_{max} is smaller (27.0 mm), the tensile stresses at both sides of the specimen lead rapidly to a serious deterioration.

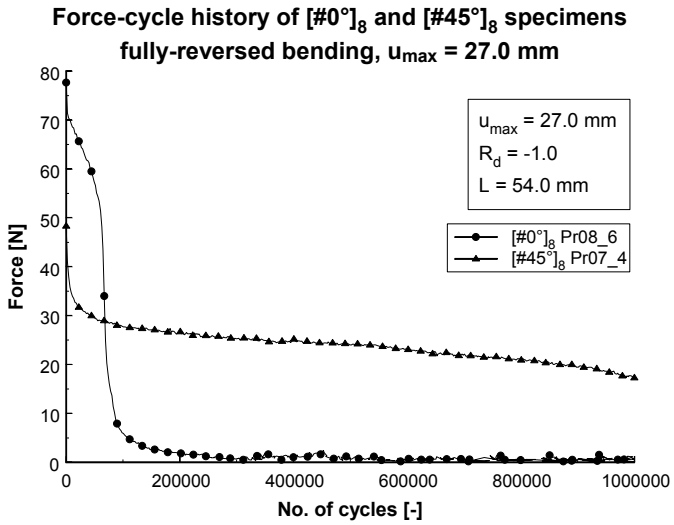

Figure 10 **Force-cycle histories for $[\#0°]_8$ and $[\#45°]_8$ specimens (fully-reversed bending R_d = -1.0, u_{max} = 27.0 mm).**

5. Local damage model

In the previous paragraph, it has been clearly demonstrated that the gradual deterioration of a fibre-reinforced composite – with a typical loss of stiffness in the damaged zones – leads to a continous redistribution of stresses and strains, and to a reduction of stress concentrations inside a structural component. Therefore a residual stiffness model is adopted here to simulate the fatigue damage behaviour of the composite specimens. In previous work of the authors [15,16], it has been shown that a fatigue damage model, similar to the one proposed by Sidoroff and Subagio [17], is capable of simulating the fatigue damage behaviour of the composite specimens:

$$\frac{dD}{dN} = \begin{cases} \dfrac{A \cdot \left(\dfrac{\Delta\sigma}{\sigma_{TS}}\right)^c}{(1-D)^b} & \text{in tension} \\ 0 & \text{in compression} \end{cases} \tag{4}$$

where:
- D : local damage variable
- N : number of cycles
- $\Delta\sigma$: amplitude of the applied cyclic loading
- σ_{TS} : tensile strength
- A, b and c : three material constants

The local damage variable D is associated with the longitudinal stiffness loss. The damage value is lying between *zero* (virgin state of the material) and *one* (complete failure of the material). The stresses and strains are related by the commonly used equation in damage mechanics (with E_0 being the undamaged modulus):

$$\sigma = E_0.(1-D).\varepsilon \tag{5}$$

The assumption that damage is not growing in the regions subjected to compressive stresses, is justified because no micro-buckling or any macroscopically significant damage could be observed at the surface that was subjected to compressive stresses.

6. Finite element analysis

The finite element implementation of the fatigue damage model deals with two important, but contradictory demands:

- in order to correctly predict the damage and residual stiffness of the composite construction after a certain number of cycles, the simulation should trace the complete path of successive damage states to keep track of the continuous stress redistribution,
- as it is impossible to simulate each of the hundreds of thousands of loading cycles for a real construction, or even for a part of it, the finite element calculations should be fast and computationally efficient.

To meet both requirements, the authors have chosen to adopt a '*cycle jump*' approach, which means that the computation is done for a certain set of loading cycles at deliberately chosen intervals, and that the effect on the stiffness degradation of these loading cycles is extrapolated over the corresponding intervals in an appropriate manner. Figure 11 illustrates the '*cycle jump*' principle.

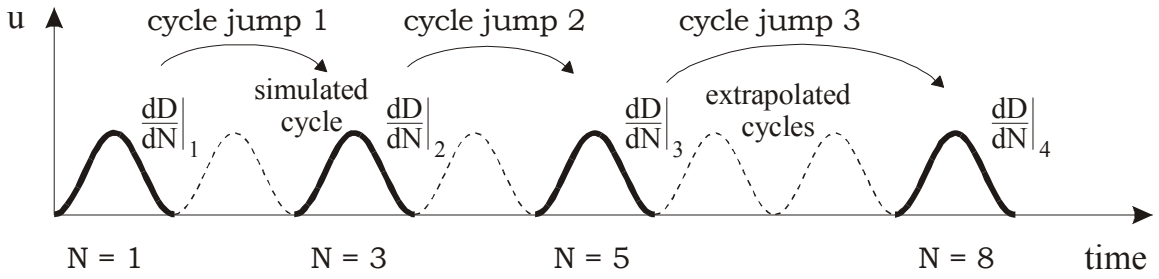

Figure 11 Illustration of the 'cycle jump' principle.

To this purpose, each Gauss-point has been assigned – beside the damage variable D – a second state variable 'NJUMP1', which is the number of cycles that could be jumped over without losing reliability and accuracy for that particular Gauss-point. After looping over all the Gauss-points, a cumulative relative frequency distribution of the 'NJUMP1' values is calculated and the overall cycle jump 'NJUMP' (which will be applied to the whole finite element mesh) is determined as a fractile of this frequency distribution.

Figure 12 shows the results of the experimental data and the finite element simulation for a $[\#45°]_8$ specimen, subjected to single-sided bending with u_{max} = 32.3 mm.

The local cycle jump 'NJUMP1' is defined by imposing a maximum increase in damage dD/dN for each particular Gauss-point when the calculation would proceed for 'NJUMP1' cycles. When the increase dD/dN is limited to for example 0.01, this is equivalent to a stepwise integration of the damage evolution law for that Gauss-point by dividing the ordinate axis of the damage-cycle history into 100 segments. By decreasing the upper threshold for dD/dN for each Gauss-point, the damage evolution law dD/dN will be integrated more accurately, but the global 'NJUMP' – a fractile of the cumulative frequency distribution of all 'NJUMP1' values – will be smaller and the calculation will proceed more slowly.

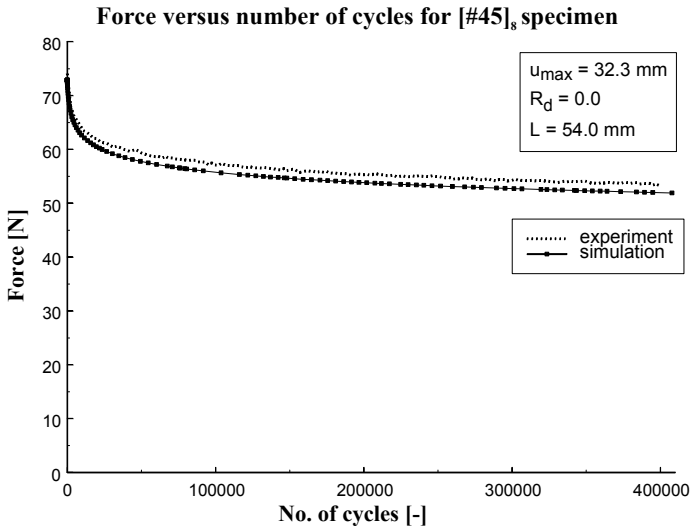

Figure 12 Experimental results versus finite element simulation for a $[\#45^o]_8$ composite specimen.

The finite element approach was implemented in the commercial finite element code SAMCEF^{TM} and the simulations were done on a Sun Workstation. The calculation shown in Figure 12, has lasted four hours and only 107 cycle jumps (i.e. finite element runs) were necessary to simulate the 400,000 loading cycles.
When the distribution of normal stress in the clamped cross-section of the composite specimen is plotted for increasing numbers of loading cycles (Figure 13), it is seen that damage, and as a consequence stiffness loss, is affecting the stress distribution in the clamped cross-section.

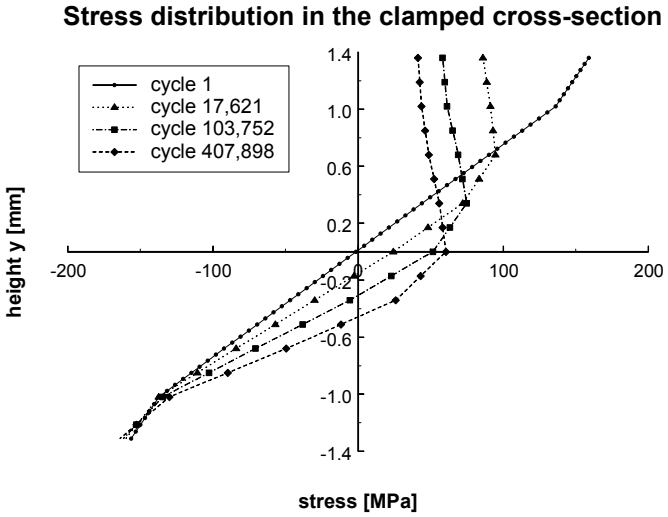

Figure 13 Distribution of the normal stresses in the clamped cross-section from finite element results.

The Figures 14 and 15 finally show the damage distribution and growth during fatigue life, as calculated by the finite element code. The abscissa coincides with the length axis of the specimen (54.0 mm), while the ordinate axis represents the thickness of the specimen (2.72 mm), so that the plot area covers the complete cross-section of the free specimen length, as

schematically indicated by the diagonal dashed lines. The contours are lines of equal damage values, where the value of the damage state variable is in the range [0,1].

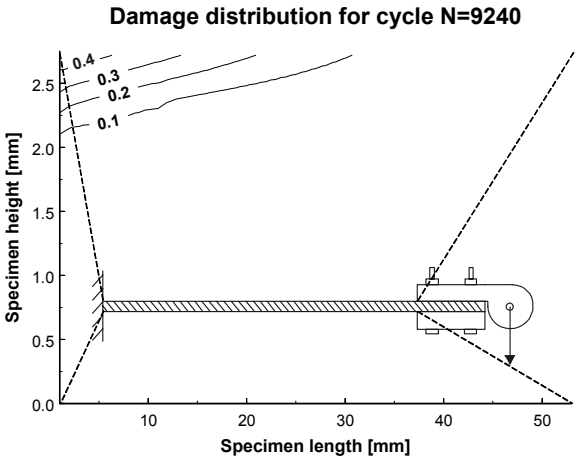

Figure 14 Damage distribution for N=9420

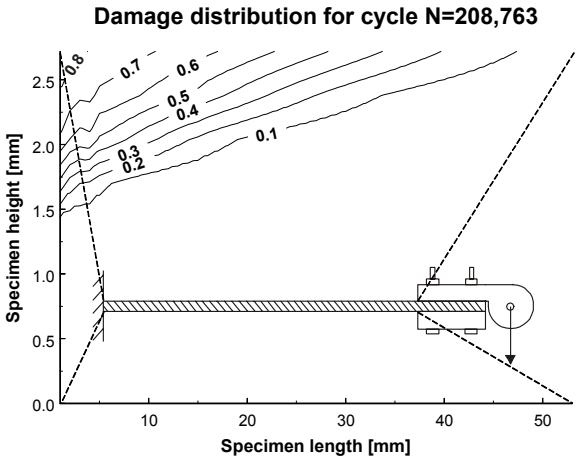

Fi gure 15 Damage distribution for N=208,763

7. Conclusions

Bending fatigue tests have been applied to plain woven glass/epoxy specimens. During the experiments, the force was measured by a strain gauge bridge and the out-of-plane displacement profile was recorded with the aid of a digital phase-shift shadow Moiré technique. These measurements provided valuable results for the development of fatigue damage models and revealed a very different behaviour between $[\#0°]_8$ and $[\#45°]_8$ stacking sequences for the glass fabric. Results from single-sided and fully-reversed bending tests have been presented.

A new finite element approach was used to implement a residual stiffness model which describes the stiffness degradation and inherent stress redistribution in the composite component. The finite element method simulates one loading cycle and then jumps over a certain number of cycles towards a new loading cycle where stiffness properties and damage distribution are altered, taking into account the effect on damage and stiffness of the cycles in between the two simulated loading cycles. The finite element implementation proves to be capable of simulating the observed force-cycle histories and stress redistribution due to stiffness degradation.

Acknowledgements

The author W. Van Paepegem gratefully acknowledges his finance through a grant of the Fund for Scientific Research – Flanders (F.W.O.), and the advice and technical support of the SAMTECH company. The authors also express their gratitude to Syncoglas for their support and technical collaboration.

References

[1] Sol H, de Wilde WP. Identification of elastic properties of composite materials using resonant frequencies. In: Proceedings of the International Conference "Computer Aided Design in Composite Material Technology". Southampton, 1988. p.273-280.

[2] Sol H. Identification of the complex moduli of composite materials by a mixed numerical/experimental method. In: Proceedings of the second International Conference on Computer Aided Design in Composite Material Technology. Brussels, April, 1990. p.267-279.

[3] Fujii T, Amijima S., Okubo K. Microscopic fatigue processes in a plain-weave glass-fibre composite. Composites Science and Technology 1993;49:327-333.

[4] Schulte K, Reese E, Chou TW. Fatigue behaviour and damage development in woven fabric and hybrid fabric composites. In: Proceedings of the Sixth International Conference on Composite Materials (ICCM-VI) & Second European Conference on Composite Materials (ECCM-II): Volume 4. London, July, 1987. p.4.89-4.99.

[5] Hansen U. Damage development in woven fabric composites during tension-tension fatigue. In: Proceedings of the 18th Risø International Symposium on Materials Science. Roskilde, September, 1997. p.345-351.

[6] Ferry L, Gabory D, Sicot N, Berard JY, Perreux D, Varchon D. Experimental study of glass-epoxy composite bars loaded in combined bending and torsion loads. Fatigue and characterisation of the damage growth. In: Proceedings of the International Conference on fatigue of composites. Paris, June, 1997. p. 266-273.

[7] Herrington PD, Doucet AB. Progression of bending fatigue damage around a discontinuity in glass/epoxy composites. Journal of Composite Materials 1992;26(14):2045-2059.

[8] Chen AS, Matthews FL. Biaxial flexural fatigue of composite plates. In: Proceedings of the Ninth International Conference on Composite Materials. Volume VI, Madrid, July, 1993. p.899-906.

[9] Manger CIC, Ogin SL, Smith PA, Greaves RP. Damage development in plain weave GFRP. In: Proceedings of the Eleventh International Conference on Composite Materials (ICCM/11), Gold Coast, July, 1997. p.V.58-V.66.

[10] Dirckx JJ, Decraemer WF, Dielis G. Phase shift method based on object translation for full field automatic 3-D surface reconstruction from moire topograms. Applied Optics 1988;27(6):1164-1169.

[11] Yoshizawa T, Tomisawa T. Shadow moiré topography by means of the phase-shift method. Optical Engineering 1993;32(7):1668-1674.

[12] Meadows DM, Johnson WO, Allen JB. Generation of surface contours by moiré patterns. Applied Optics 1970;9(4):942-947.

[13] Kujawinska M, Osten W. Fringe pattern analysis methods: up-to-date review. In: Proceedings SPIE 1998;3407:56-66.

[14] Kreis T. Holographic interferometry - Principles and methods. Berlin: Akademie Verlag, 1996.

[15] Van Paepegem W, Degrieck, J. Experimental setup for the bending fatigue of fibre-

reinforced composite materials. In: Proceedings of Fatigue. Cambridge, April, 2000. p.115-122.

[16] Van Paepegem W, Degrieck J. Experimental setup for and numerical modelling of bending fatigue experiments on plain woven glass/epoxy composites. Accepted for publication in Composite Structures.

[17] Sidoroff F, Subagio B. Fatigue damage modelling of composite materials from bending tests. In: Proceedings of the Sixth International Conference on Composite Materials (ICCM-VI) & Second European Conference on Composite Materials (ECCM-II): Volume 4. London, July, 1987. p.4.32-4.39.